SCIENCE CHINA
Information Sciences

• RESEARCH PAPER •

October 2017, Vol. 60 102306:1–102306:13
doi: 10.1007/s11432-016-0611-x

Throughput and BER of wireless powered DF relaying in Nakagami-m fading

Yan GAO[1], Yunfei CHEN[2*] & Aiqun HU[3]

[1]*School of Electronic Information, Nanjing College of Information Technology, Nanjing* 210023*, China;*
[2]*College of Computer and Information, Hohai University, Nanjing* 211100*, China;*
[3]*College of Information Science and Engineering, Southeast University, Nanjing* 210096*, China*

Received September 14, 2016; accepted November 21, 2016; published online June 28, 2017

Abstract Energy harvesting provides a promising solution to the extra energy requirement at the relay due to relaying. In this paper, the throughput and bit error rate of a decode-and-forward relaying system are studied using power splitting wireless power. Three different transmission scenarios are considered: instantaneous transmission, delay- or error-constrained transmission and delay- or error-tolerant transmission. For each scenario, exact expressions for the throughput and bit error rate are derived. Numerical results show that, for instantaneous transmission, the optimum splitting factor is not sensitive to the channel gain of the source-to-relay link. For delay- or error-constrained transmissions, the optimum splitting factor increases with the quality of the source-to-relay link and decreases with the quality of the relay-to-destination link. For delay- or error-tolerant transmissions, the optimum splitting factor is insensitive to the quality of the source-to-relay link.

Keywords decode-and-forward, energy harvesting, power-splitting, relaying

Citation Gao Y, Chen Y F, Hu A Q. Throughput and BER of wireless powered DF relaying in Nakagami-m fading. Sci China Inf Sci, 2017, 60(10): 102306, doi: 10.1007/s11432-016-0611-x

1 Introduction

Decode-and-forward (DF) is an effective method of relaying [1]. On the other hand, energy harvesting is becoming a practical solution to low-power applications. In [2], two practical schemes that use time-switching (TS) and power-splitting (PS) were proposed. In the TS scheme, the receiver alternates between harvesting time and decoding time and thus, the throughput is reduced due to the extra harvesting time. Also, since the receiver uses the same components to process energy and information, its hardware is limited due to the huge difference between the energy sensitivity and the information sensitivity. The PS scheme splits a portion of the received signal for harvesting and processes energy and information using separate components to avoid these problems. Thus, in this paper, PS is considered.

Previous works on energy harvesting DF relaying mainly include the following. In [3], the effect of random location of the relay on the outage probability of DF relaying using PS wireless power was studied for Rayleigh fading channels. In [4], the approximate ergodic capacity of the DF relaying using TS and PS were investigated for Rayleigh fading channels. A literature review of relevant wireless powered relaying

* Corresponding author (email: Yunfei.Chen@warwick.ac.uk)

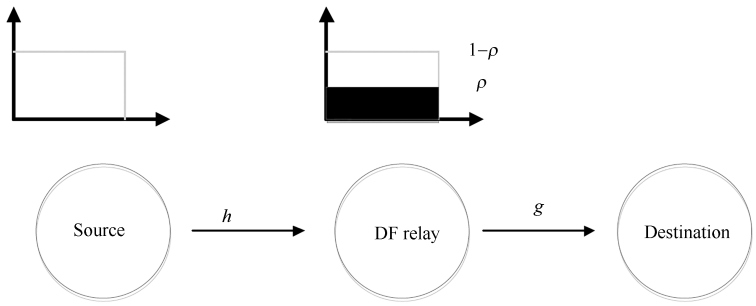

Figure 1 A diagram of the considered system.

can be found in [5]. Ref. [6] analyzed the throughput of a DF relaying system using energy harvesting. Ref. [7] considered the nonlinear distortion and imperfect channel information in the analysis. In [8], the throughput of a DF relaying system with multiple antennas was analyzed and maximized. Ref. [9] considered full-duplex radios in the system. Ref. [10] conducted a similar study by considering both PS and TS. Also, Ref. [11] used game theories for the precoding design of a DF energy harvesting relaying system. Further, Ref. [12] designed new noncoherent receivers for energy harvesting DF systems. Finally, Ref. [13] considered the use of multiple hops instead of two hops and compared the efficiency for different relaying schemes. All these works have provided very useful insights into the design of DF relaying using wireless power. However, there lacks a comprehensive performance analysis for such a system, which is the purpose of this paper.

In this paper, the exact bit error rate (BER) and throughput of DF relaying are analyzed assuming PS wireless power in Nakagami-m fading channels. Three different scenarios are considered: instantaneous transmission where the channel state information is known, delay- or error-constrained where the source transmission rate or the error rate are restricted by a minimum requirement, and delay- or error-tolerant where throughput or error rate are averaged over the channel state. For each scenario, the exact expressions for the end-to-end bit error rate and the end-to-end-throughput are derived. Numerical results show that, for instantaneous transmission, the optimum splitting factor does not depend on the channel gain of the source-to-relay link. For delay- or error-constrained transmissions, the optimum splitting factor increases with the average fading power of the source-to-relay link and decreases with the average fading power of the relay-to-destination link. For delay- or error-tolerant transmissions, the optimum splitting factor is less sensitive to the source-to-relay link than to the relay-to-destination link.

2 System model

In this paper, a DF relaying system consisting of a source, a relay and a destination, is considered. Each node is half-duplex and has a single antenna. The source transmits a signal to the relay. The relay splits the received signal into two parts. One part is used for energy harvesting and the other part is used for information decoding. The decoded information is then encoded again and forwarded to the destination by using the harvested energy. Figure 1 shows a diagram of the considered system. Assume a total relaying time of T, where $T/2$ is spent in the source-to-relay link and $T/2$ is spent in the relay-to-destination link. There is no direct link between the source and the destination. This is the case when the destination is out of the transmission range of the source or the destination is obstructed from the source [14, 15].

Using the above assumptions, the received signal for information decoding at the relay can be expressed as

$$y_k^r = \sqrt{(1-\rho)\frac{P_S}{d_s^v}}ha + \sqrt{1-\rho}n_k^{ra} + n_k^{rc}, \tag{1}$$

where P_S is the transmitted power of the source, ρ is the PS factor to be optimized, d_s is the distance between source and relay, v is the path loss exponent, h is the Nakagami-m fading gain of the source-to-

relay link, a is the transmitted symbol with unit average power, n_k^{ra} is the k-th sample of the noise from the antenna and n_k^{rc} is the k-th sample of the noise from the RF-to-baseband conversion. Also, h is the Nakagami-m fading gain such that $|h|^2$ follows a Gamma distribution with probability density function (PDF) of

$$f_{|h|^2}(x) = \left(\frac{m_1}{\Omega_1}\right)^{m_1} \frac{x^{m_1-1}}{\Gamma(m_1)} \mathrm{e}^{-\frac{m_1}{\Omega_1}x}, \quad x > 0, \tag{2}$$

where m_1 is the Nakagami-m parameter with $m_1 \leqslant 0.5$ and Ω_1 is the average fading power of the source-to-relay link, and $\Gamma(\cdot)$ is the complete Gamma function [16, Eq. (8.310.1)]. The noise samples n_k^{ra} and n_k^{rc} are assumed to be additive white Gaussian noise (AWGN) with mean zero and variance σ_{ra}^2 and σ_{rc}^2, respectively, and are independent of each other. Also, all the noise samples are circularly symmetric in this paper.

Thus, the transmission power of the relay using the harvested energy is

$$P_r = \frac{E_h}{T/2} = \eta\rho \frac{P_S}{d_s^v}|h|^2, \tag{3}$$

where η is the conversion efficiency of the energy harvester equipped at the relay.

Using the harvested energy at the relay, the received signal at the destination can be given by

$$y_k^d = \sqrt{\frac{P_r}{d_r^v}} gb + n_k^{da} + n_k^{dc}, \tag{4}$$

where P_r is the transmission power of the relay given in (3), d_r is the distance between relay and destination, g is the Nakagami-m fading gain of the relay-to-destination link, b is the symbol transmitted by the relay also with unit average power, and n_k^{da} and n_k^{dc} are the antenna noise and the conversion noise, respectively. The channel gain g suffers from Nakagami-m fading such that $|g|^2$ follows a Gamma distribution with PDF:

$$f_{|g|^2}(x) = \left(\frac{m_2}{\Omega_2}\right)^{m_2} \frac{x^{m_2-1}}{\Gamma(m_2)} \mathrm{e}^{-\frac{m_2}{\Omega_2}x}, \quad x > 0, \tag{5}$$

where m_2 is the Nakagami-m parameter with $m_2 \leqslant 0.5$ and Ω_2 is the average fading power of the relay-to-destination link. The noise samples n_k^{da} and n_k^{dc} are assumed to be AWGN with mean zero and variance σ_{da}^2 and σ_{dc}^2, respectively, and are independent of each other.

For later use, the cumulative distribution functions (CDFs) of $|h|^2$ and $|g|^2$ are given by

$$F_{|h|^2}(y) = \frac{\gamma(m_1, \frac{m_1}{\Omega_1}y)}{\Gamma(m_1)}, \quad y > 0, \tag{6}$$

$$F_{|g|^2}(y) = \frac{\gamma(m_2, \frac{m_2}{\Omega_2}y)}{\Gamma(m_2)}, \quad y > 0, \tag{7}$$

respectively, where $\gamma(\cdot,\cdot)$ is the lower incomplete Gamma function [16, Eq. (8.350.1)].

Using (1) and (4), the BERs for binary phase shift keying (BPSK) at the relay and at the destination are [17]

$$\mathrm{BER}_r = \frac{1}{2}\mathrm{erfc}(\sqrt{\gamma_1}), \tag{8}$$

$$\mathrm{BER}_d = \frac{1}{2}\mathrm{erfc}(\sqrt{\gamma_2}), \tag{9}$$

respectively, where $\gamma_1 = \frac{(1-\rho)P_S|h|^2/d_s^v}{(1-\rho)\sigma_{ra}^2+\sigma_{rc}^2}$ is the instantaneous signal-to-noise ratio (SNR) of the source-to-relay link, $\gamma_2 = \frac{\eta\rho P_S|h|^2|g|^2/(d_s^v d_r^v)}{\sigma_{da}^2+\sigma_{dc}^2}$ is the instantaneous SNR of the relay-to-destination link, and $\mathrm{erfc}(\cdot)$ is the complementary error function [16, Eq. (8.250.4)]. In this case, the transmitted symbol b in (4) is given by $b = \mathrm{sign}(y_k^r h^*)$, where $\mathrm{sign}(\cdot)$ is the signum function and $*$ is the conjugate operation. Similarly, the throughputs of the source-to-relay link and the relay-to-destination link are [4, 5]

$$C_r = \ln(1+\gamma_1), \tag{10}$$

$$C_d = \ln(1+\gamma_2). \tag{11}$$

3 Throughput and BER analysis

3.1 Instantaneous transmission

In this scenario, the channel state information is known through channel estimation. Thus, the end-to-end BER of the relaying link is [18]

$$\mathrm{BER} = \mathrm{BER}_r(1-\mathrm{BER}_d) + \mathrm{BER}_d(1-\mathrm{BER}_r). \tag{12}$$

This equation omits the case when both hops contain errors, as this is negligible for a properly designed communications link [18]. For example, for properly designed links, $\mathrm{BER}_r = 10^{-5}$ and $\mathrm{BER}_d = 10^{-5}$. Thus, $\mathrm{BER}_r * \mathrm{BER}_d = 10^{-10}$, much smaller than the other cases. Using (8) and (9), one has

$$\begin{aligned}\mathrm{BER} =& \frac{1}{2}\mathrm{erfc}\left(\sqrt{\frac{(1-\rho)P_S|h|^2/d_s^v}{(1-\rho)\sigma_{ra}^2+\sigma_{rc}^2}}\right) + \frac{1}{2}\mathrm{erfc}\left(\sqrt{\frac{\eta\rho P_S|h|^2|g|^2/(d_s^v d_r^v)}{\sigma_{da}^2+\sigma_{dc}^2}}\right)\\ &- \frac{1}{2}\mathrm{erfc}\left(\sqrt{\frac{(1-\rho)P_S|h|^2/d_s^v}{(1-\rho)\sigma_{ra}^2+\sigma_{rc}^2}}\right)\mathrm{erfc}\left(\sqrt{\frac{\eta\rho P_S|h|^2|g|^2/(d_s^v d_r^v)}{\sigma_{da}^2+\sigma_{dc}^2}}\right).\end{aligned} \tag{13}$$

The optimization problem is to find the optimum value of ρ that minimizes BER for $0<\rho<1$, $P_S>0$, $0<\eta<1$, $d_r>0$ and $d_s>0$. One sees that the third term in (13) is very small compared with the first two terms and can be ignored. In this case, the overall BER decreases when $P_s|h|^2$, $|g|^2$, η increase, or when the path loss d_s^v, d_r^v or the noise power $\sigma_{da}^2+\sigma_{dc}^2$, $(1-\rho)\sigma_{ra}^2+\sigma_{rc}^2$ decrease, as expected.

On the other hand, the end-to-end throughput of the DF relaying system can be derived as [4]

$$C = \min\{C_r, C_d\} = \ln\left(1+\min\left\{\frac{(1-\rho)P_S|h|^2/d_s^v}{(1-\rho)\sigma_{ra}^2+\sigma_{rc}^2}, \frac{\eta\rho P_S|h|^2|g|^2/(d_s^v d_r^v)}{\sigma_{da}^2+\sigma_{dc}^2}\right\}\right). \tag{14}$$

Similarly, from (14), the throughput increases when $P_s|h|^2$, $|g|^2$, η increase, or when the path loss d_s^v, d_r^v or the noise power $\sigma_{da}^2+\sigma_{dc}^2$, $(1-\rho)\sigma_{ra}^2+\sigma_{rc}^2$ decrease.

To find the optimum value of ρ, one needs to decide which SNR is the smaller one, that is,

$$\frac{(1-\rho)P_S|h|^2/d_s^v}{(1-\rho)\sigma_{ra}^2+\sigma_{rc}^2} <> \frac{\eta\rho P_S|h|^2|g|^2/(d_s^v d_r^v)}{\sigma_{da}^2+\sigma_{dc}^2}, \tag{15}$$

where $<>$ indicates the relationship to be determined. This leads to a quadratic equation of ρ. Its discriminant can be calculated as

$$\Delta = \left[\eta\frac{|g|^2}{d_r^v}\sigma_{rc}^2\right]^2 + 2\left(\eta\frac{|g|^2}{d_r^v}\sigma_{rc}^2\right)\left(\sigma_{da}^2+\sigma_{dc}^2+\eta\frac{|g|^2}{d_r^v}\sigma_{ra}^2\right) + \left(\sigma_{da}^2+\sigma_{dc}^2-\eta\frac{|g|^2}{d_r^v}\sigma_{ra}^2\right)^2 > 0, \tag{16}$$

and it has two roots, one of which is larger than 1 and can be ignored. Using the root that is smaller than 1 and denoted as ρ_1, when $0 \leqslant \rho < \rho_1$, one has

$$\frac{(1-\rho)P_S|h|^2/d_s^v}{(1-\rho)\sigma_{ra}^2+\sigma_{rc}^2} > \frac{\eta\rho P_S|h|^2|g|^2/(d_s^v d_r^v)}{\sigma_{da}^2+\sigma_{dc}^2}, \tag{17}$$

such that

$$C = \ln\left(1+\frac{\eta\rho P_S|h|^2|g|^2/(d_s^v d_r^v)}{\sigma_{da}^2+\sigma_{dc}^2}\right), \tag{18}$$

and when $\rho_1 \leqslant \rho \leqslant 1$, one has

$$\frac{(1-\rho)P_S|h|^2/d_s^v}{(1-\rho)\sigma_{ra}^2+\sigma_{rc}^2} < \frac{\eta\rho P_S|h|^2|g|^2/(d_s^v d_r^v)}{\sigma_{da}^2+\sigma_{dc}^2}, \tag{19}$$

such that

$$C = \ln\left(1+\frac{(1-\rho)P_S|h|^2/d_s^v}{(1-\rho)\sigma_{ra}^2+\sigma_{rc}^2}\right). \tag{20}$$

In both cases, the maximum value of C is achieved when $\rho = \rho_1$. Thus, the optimum value of ρ is given by

$$\rho_{\text{opt}}^{C} = \frac{\left(\sigma_{da}^2 + \sigma_{dc}^2 + \eta\frac{|g|^2}{d_r^v}\sigma_{rc}^2 + \eta\frac{|g|^2}{d_r^v}\sigma_{ra}^2\right) - \sqrt{\Delta}}{2\eta\frac{|g|^2}{d_r^v}\sigma_{ra}^2}, \tag{21}$$

where $\Delta = \left[\eta\frac{|g|^2}{d_r^v}\sigma_{rc}^2\right]^2 + 2\left(\eta\frac{|g|^2}{d_r^v}\sigma_{rc}^2\right)\left(\sigma_{da}^2 + \sigma_{dc}^2 + \eta\frac{|g|^2}{d_r^v}\sigma_{ra}^2\right) + \left(\sigma_{da}^2 + \sigma_{dc}^2 - \eta\frac{|g|^2}{d_r^v}\sigma_{ra}^2\right)^2$. Several insights can be gained. First, from (21), the optimum value of ρ does not depend on $|h|^2$, suggesting that it will not be sensitive to the quality of the source-to-relay link in setting up ρ. Second, when $\frac{|g|^2/d_r^v}{\sigma_{da}^2+\sigma_{dc}^2}$ goes to infinity, ρ_{opt}^{C} approaches zero, indicating that less power should be harvested when the relay-to-destination link is good. Third, the product term in (13) can be ignored to simplify the expression. In this case, the BER decreases with $|h|^2$ and $|g|^2$. Also, as ρ increases, the first term increases while the second term decreases, leading to optimum BER. Note that this case represents a fading channel with known channel state information, not a static channel, although the result is applicable to a static channel as well.

3.2 Delay- or error-constrained

In this scenario, the transmission rate of the source or the bit error rate are restricted by a minimum requirement. Specifically, for the delay-constrained case, one has $C = R_0$ such that the throughput is constrained by

$$\hat{C} = \frac{R_0}{2}\left(1 - p_{\text{out}}^{C}\right), \tag{22}$$

where $1/2$ takes the throughput penalty of relaying into account, $p_{\text{out}}^{C} = \Pr\{\gamma < \gamma_{th}^{C}\}$ and $\gamma = \min\{\gamma_1, \gamma_2\}$ $= \min\left\{\frac{(1-\rho)P_S|h|^2/d_s^v}{(1-\rho)\sigma_{ra}^2+\sigma_{rc}^2}, \frac{\eta\rho P_S|h|^2|g|^2/(d_s^v d_r^v)}{\sigma_{da}^2+\sigma_{dc}^2}\right\}$ being the end-to-end SNR of the DF relaying system and $\gamma_{th}^{C} = 2^{R_0} - 1$ is the threshold of γ.

Similarly, for the error-constrained case, one has $\text{BER} = \text{BER}_r(1-\text{BER}_d)+\text{BER}_d(1-\text{BER}_r) = \text{BER}_0$. However, this form is not convenient, as it is difficult to calculate the inverse function using this form. Instead, we use $\text{BER} = \frac{1}{2}\text{erfc}\left(\sqrt{\gamma_{eq}}\right)$, where $\gamma - 1.62 < \gamma_{eq} \leqslant \gamma$ is the equivalent end-to-end SNR in the sense of BER [18] and γ is the original end-to-end SNR. Thus, one has $\frac{1}{2}\text{erfc}(\sqrt{\gamma_{eq}}) < \text{BER}_0$ such that $\gamma_{eq} > \gamma_{th}^{B}$, where $\gamma_{th}^{B} = \left[\text{erfc}^{-1}(2\text{BER}_0)\right]^2$ and $\text{erfc}^{-1}(\cdot)$ is the inverse function of the complementary error function. To be consistent with (22), the bit correct rate (BCR) is constrained as

$$\hat{\text{BCR}} = (1 - \text{BER}_0)\left(1 - p_{\text{out}}^{B}\right), \tag{23}$$

where $p_{\text{out}}^{B} = \Pr\left\{\gamma < \gamma_{th}^{B}\right\}$ or $p_{\text{out}}^{B} = \Pr\left\{\gamma < \gamma_{th}^{B} + 1.62\right\}$.

Thus, the derivations of the constrained throughput and BCR boil down to the calculation of the CDF of γ. Starting from the definition of the CDF, one has

$$\begin{aligned} F_\gamma(y) =& \Pr\left\{\frac{\sigma_{da}^2 + \sigma_{dc}^2}{(1-\rho)\sigma_{ra}^2 + \sigma_{rc}^2}\frac{1-\rho}{\eta\rho}d_r^v < |g|^2,\ \frac{(1-\rho)P_S|h|^2/d_s^v}{(1-\rho)\sigma_{ra}^2 + \sigma_{rc}^2} < y\right\} \\ &+ \Pr\left\{\frac{\sigma_{da}^2 + \sigma_{dc}^2}{(1-\rho)\sigma_{ra}^2 + \sigma_{rc}^2}\frac{1-\rho}{\eta\rho}d_r^v > |g|^2,\ \frac{\eta\rho P_S|h|^2|g|^2/(d_s^v d_r^v)}{\sigma_{da}^2 + \sigma_{dc}^2} < y\right\}. \end{aligned} \tag{24}$$

Assuming that h is independent of g, this can be derived as

$$\begin{aligned} F_\gamma(y) =& F_{|g|^2}\left(\frac{\sigma_{da}^2 + \sigma_{dc}^2}{(1-\rho)\sigma_{ra}^2 + \sigma_{rc}^2}\frac{1-\rho}{\eta\rho}d_r^v\right) + F_{|h|^2}\left(\frac{(1-\rho)\sigma_{ra}^2 + \sigma_{rc}^2}{(1-\rho)P_S}d_s^v y\right) \\ &- F_{|g|^2}\left(\frac{\sigma_{da}^2 + \sigma_{dc}^2}{(1-\rho)\sigma_{ra}^2 + \sigma_{rc}^2}\frac{1-\rho}{\eta\rho}d_r^v\right)F_{|h|^2}\left(\frac{(1-\rho)\sigma_{ra}^2 + \sigma_{rc}^2}{(1-\rho)P_S}d_s^v y\right) \\ &- \frac{m_2}{\Omega_2}\frac{1}{\Gamma(m_2)}\sum_{l=0}^{m_1-1}\frac{\left(\frac{m_1(\sigma_{da}^2+\sigma_{dc}^2)}{\Omega_1\eta\rho P_S}d_s^v y\right)^l}{l!} \end{aligned}$$

$$\int_0^{\frac{\sigma_{da}^2+\sigma_{dc}^2}{(1-\rho)\sigma_{ra}^2+\sigma_{rc}^2}\frac{1-\rho}{\eta\rho}d_r^v} t^{m_2-1-l}\mathrm{e}^{-\frac{m_2}{\Omega_2}t-\frac{m_1(\sigma_{da}^2+\sigma_{dc}^2)d_s^v y}{\Omega_1\eta\rho P_S t}}\mathrm{d}t, \tag{25}$$

where $F_{|h|^2}(\cdot)$ and $F_{|g|^2}(\cdot)$ are the CDFs of $|h|^2$ and $|g|^2$ given in (6) and (7), respectively. Using (25), one has

$$\hat{C} = \frac{R_0}{2}\left[1 - F_\gamma(\gamma_{th}^C)\right], \tag{26}$$

and

$$\hat{\mathrm{BCR}} = (1-\mathrm{BER}_0)\left[1 - F_\gamma(\gamma_{th}^B)\right], \text{ or } \hat{\mathrm{BCR}} = (1-\mathrm{BER}_0)\left[1 - F_\gamma(\gamma_{th}^B + 1.62)\right]. \tag{27}$$

One observes that $\hat{C}$ and $\hat{\mathrm{BCR}}$ increase when $F_\gamma(\gamma_{th}^C)$ decreases. Eq. (25) can be simplified by removing the last term when the signal-to-noise ratios are large. Also, from (25), one can see that the performance improves when P_S increases, d_s^v decreases, or d_r^v decreases.

3.3 Delay- or error-tolerant

This scenario applies to applications with no minimum requirement on quality of service. In the case of delay-tolerant, the ergodic capacity can be calculated as

$$\bar{C} = \int_0^\infty\int_0^\infty \ln\left(1+\min\left\{\frac{P_S x/d_s^v}{\sigma_{ra}^2+\frac{\sigma_{rc}^2}{(1-\rho)}}, \frac{\eta\rho P_S xy/(d_s^v d_r^v)}{\sigma_{da}^2+\sigma_{dc}^2}\right\}\right) f_{|h|^2,|g|^2}(x,y)\mathrm{d}x\mathrm{d}y, \tag{28}$$

and is derived in Appendix A as

$$\begin{aligned}\bar{C} = &\left[1 - F_{|g|^2}\left(\frac{\sigma_{da}^2+\sigma_{dc}^2}{(1-\rho)\sigma_{ra}^2+\sigma_{rc}^2}\frac{1-\rho}{\eta\rho}d_r^v\right)\right]\frac{(m_1/\Omega_1)^{m_1}}{\Gamma(m_1)}\\ &\cdot W\left(\frac{(1-\rho)P_S/d_s^v}{(1-\rho)\sigma_{ra}^2+\sigma_{rc}^2}, m_1, \frac{m_1}{\Omega_1}\right)\\ &+\frac{(\frac{m_1}{\Omega_1})^{m_1}}{\Gamma(m_1)}\frac{(\frac{m_2}{\Omega_2})^{m_2}}{\Gamma(m_2)}\int_0^{\frac{\sigma_{da}^2+\sigma_{dc}^2}{(1-\rho)\sigma_{ra}^2+\sigma_{rc}^2}\frac{1-\rho}{\eta\rho}d_r^v} W\left(\frac{\eta\rho P_S y/(d_s^v d_r^v)}{\sigma_{da}^2+\sigma_{dc}^2}, m_1, \frac{m_1}{\Omega_1}\right)\\ &\cdot y^{m_2-1}\mathrm{e}^{-\frac{m_2}{\Omega_2}y}\mathrm{d}y,\end{aligned} \tag{29}$$

where

$$W(a,b,c) = \int_0^\infty \ln(1+ax)x^{b-1}\mathrm{e}^{-cx}\mathrm{d}x \tag{30}$$

$$= \frac{\mathrm{e}^{c/a}}{a^b}\sum_{i=0}^{b-1}\binom{b-1}{i}(-1)^{b-1-i}\frac{\partial}{\partial v}\left\{\left(\frac{a}{c}\right)^v\Gamma(v,c/a)\right\}\Big|_{v=i+1}, \tag{31}$$

where $\Gamma(\cdot,\cdot)$ is the upper incomplete Gamma function [16, Eq. (8.350.2)].

In the case of error-tolerant transmission, the average BER can be calculated as

$$\begin{aligned}\bar{\mathrm{BER}} = &\int_0^\infty\int_0^\infty\left[\frac{1}{2}\mathrm{erfc}\left(\sqrt{\frac{(1-\rho)P_S x/d_s^v}{(1-\rho)\sigma_{ra}^2+\sigma_{rc}^2}}\right)+\frac{1}{2}\mathrm{erfc}\left(\sqrt{\frac{\eta\rho P_S xy/(d_s^v d_r^v)}{\sigma_{da}^2+\sigma_{dc}^2}}\right)\right.\\ &\left.-\frac{1}{2}\mathrm{erfc}\left(\sqrt{\frac{(1-\rho)P_S x/d_s^v}{(1-\rho)\sigma_{ra}^2+\sigma_{rc}^2}}\right)\cdot\mathrm{erfc}\left(\sqrt{\frac{\eta\rho P_S xy/(d_s^v d_r^v)}{\sigma_{da}^2+\sigma_{dc}^2}}\right)\right] f_{|h|^2}(x)f_{|g|^2}(y)\mathrm{d}x\mathrm{d}y.\end{aligned} \tag{32}$$

This is derived in Appendix B as

$$\begin{aligned}\bar{\mathrm{BER}} = &\frac{1}{2}\frac{(m_1/\Omega_1)^{m_1}}{\Gamma(m_1)}U\left(\frac{(1-\rho)P_S/d_s^v}{(1-\rho)\sigma_{ra}^2+\sigma_{rc}^2}, m_1, \frac{m_1}{\Omega_1}\right)\\ &+\frac{1}{2}\frac{(m_1/\Omega_1)^{m_1}(m_2/\Omega_2)^{m_2}}{\Gamma(m_1)\Gamma(m_2)}V\left(\frac{\eta\rho P_S/(d_s^v d_r^v)}{\sigma_{da}^2+\sigma_{dc}^2}, m_1, \frac{m_1}{\Omega_1}, m_2, \frac{m_2}{\Omega_2}\right)\end{aligned}$$

$$-\frac{1}{2}\frac{(\frac{m_1}{\Omega_1})^{m_1}(\frac{m_2}{\Omega_2})^{m_2}}{\Gamma(m_1)\Gamma(m_2)}$$
$$\cdot\int_0^{\infty}\operatorname{erfc}\left(\sqrt{\frac{(1-\rho)P_S x/d_s^v}{(1-\rho)\sigma_{ra}^2+\sigma_{rc}^2}}\right)x^{m_1-1}\mathrm{e}^{-\frac{m_1}{\Omega_1}x}$$
$$U\left(\frac{\eta\rho P_S x/(d_s^v d_r^v)}{\sigma_{da}^2+\sigma_{dc}^2},m_2,\frac{m_2}{\Omega_2}\right)\mathrm{d}x, \tag{33}$$

where

$$U(a,b,c)=\frac{\Gamma(b)}{c^b}-\frac{2\sqrt{a}\Gamma(b+0.5)}{\sqrt{\pi}(\sqrt{c})^{2b+1}}{}_2F_1\left(0.5,b+0.5;1.5;-\frac{a}{c}\right), \tag{34}$$

and

$$V(a,b_1,c_1,b_2,c_2)=\frac{\Gamma(b_1)\Gamma(b_2)}{c_1^{b_1}c_2^{b_2}}-\frac{2\sqrt{a/\pi}\Gamma(3/2)}{c_1^{b_1+0.5}c_2^{b_2+0.5}\Gamma(0.5)\Gamma(b_1+0.5)}$$
$$E\left(0.5,b_1+0.5;b_2+0.5,1.5;\frac{c_1c_2}{a}\right), \tag{35}$$

with ${}_2F_1(\cdot,\cdot;\cdot;\cdot)$ being the hypergeometric function [16, Eq. (9.100.1)] and $E(\cdot,\cdot;\cdot,\cdot;\cdot)$ is the MacRobert's E function [16, Eq. (9.41)]. These expressions are quite complicated and do not provide many insights directly. However, they save the computational time. Also, insights can be gained by doing numerical calculations indirectly. The above results are for BPSK. It is well known that a unified expression for the BER is [17, 19]

$$\mathrm{BER}_r=\frac{a}{2}\operatorname{erfc}\left(\sqrt{\frac{b}{2}\gamma_1}\right),\ \text{or}\ \mathrm{BER}_d=\frac{a}{2}\operatorname{erfc}\left(\sqrt{\frac{b}{2}\gamma_2}\right), \tag{36}$$

where $a=1$ and $b=2$ for BPSK as discussed above, $a=1$ and $b=1$ for binary frequency shift keying, $a=2\frac{M-1}{M}$ for M-ary amplitude shift keying, $a=2$ and $b=2\sin^2(\pi/M)$ is a good approximation for M-ary phase shift keying, and M is the constellation size. Comparing (36) with (8) or (9), one can see that the results for other modulation schemes can be easily obtained by replacing a and b with relevant values. Also, the symbol SNR can be derived as a function of the bit SNR. To make this paper compact, such a straightforward extension is not made here.

4 Numerical results and discussion

In this case, the BER and throughput in three different scenarios will be examined. Without loss of generality, in the examination, $P_S=1$, $\sigma_{ra}^2 d_s^v=\sigma_{rc}^2 d_s^v=\sigma_{da}^2 d_r^v=\sigma_{dc}^2 d_r^v=1$, while $|h|^2$ and $|g|^2$ in the instantaneous transmission change with $\beta_1=\frac{|h|^2/d_s^v}{\sigma_{ra}^2+\sigma_{rc}^2}$ and $\beta_2=\frac{|g|^2/d_r^v}{\sigma_{da}^2+\sigma_{dc}^2}$ and Ω_1 and Ω_2 in the delay- and error-tolerant or -constrained transmissions change with $\beta_1=\frac{\Omega_1/d_s^v}{\sigma_{ra}^2+\sigma_{rc}^2}$ and $\beta_2=\frac{\Omega_2/d_r^v}{\sigma_{da}^2+\sigma_{dc}^2}$. The value of β_1 and β_2 can be considered as the quality indicators of the source-to-relay and relay-to-destination links. Also, the path loss effect is included in the calculation of β_1 and β_2.

Figures 2–5 show the performances of instantaneous transmission using DF relaying with PS wireless power. In particular, Figure 2 shows the throughput vs. ρ for different values of β_1, β_2 and η. Several observations can be made. First, there does exist an optimum value of ρ that maximizes the throughput, in all the cases considered, as expected. The optimum value of ρ lies at the only discontinuity of the throughput, which agrees with the derivation in Appendix A. Second, when the value of η increases, the throughput increases and the optimum value of ρ decreases, due to higher conversion efficiency, but a large part of the throughput curves overlap with each other on the right side of the peak, indicating that the throughput performance is not sensitive to the value of η in this part. This can be explained by (24) where the throughput does not depend on η. Third, when β_1 or β_2 increase, the throughput increases and it is more sensitive to β_1, as channel conditions become better. Figure 3 shows the BER vs. ρ for different values of β_1, β_2 and η. In this case, there exists an optimum value of ρ that minimizes the BER

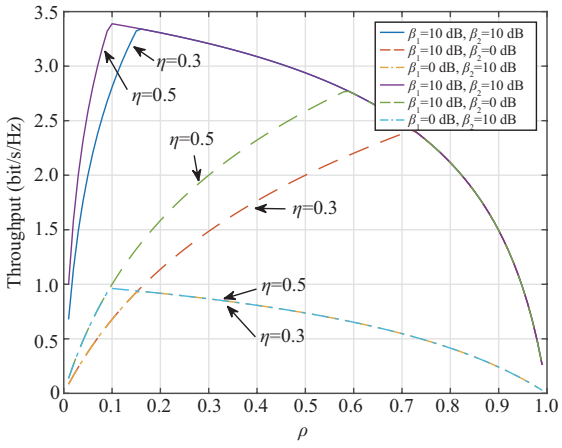

Figure 2 (Color online) Throughput vs. ρ for different values of η, β_1 and β_2 in instantaneous transmission.

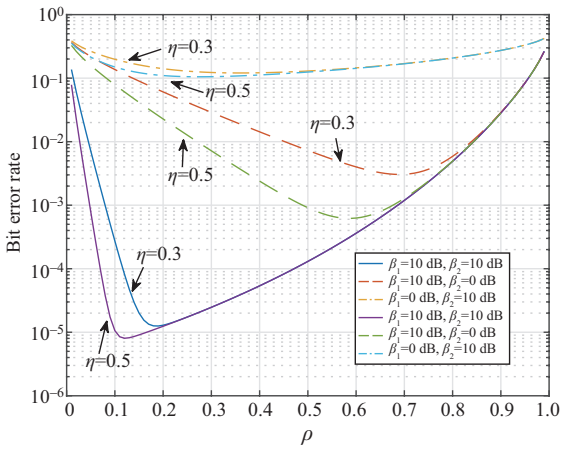

Figure 3 (Color online) BER vs. ρ for different values of η, β_1 and β_2 in instantaneous transmission.

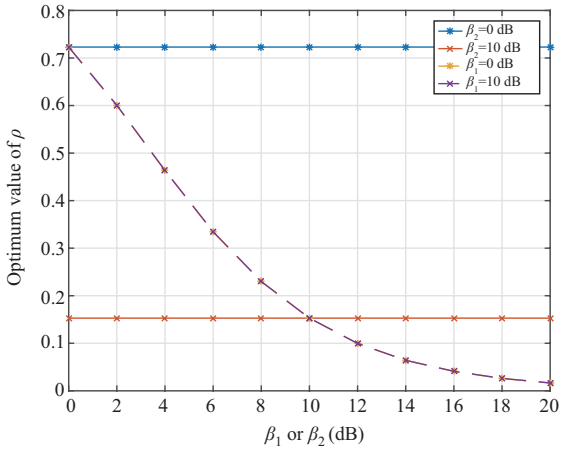

Figure 4 (Color online) The optimum value of ρ vs. β_1 or β_2 when $\eta = 0.3$ to achieve the maximum throughput in instantaneous transmission.

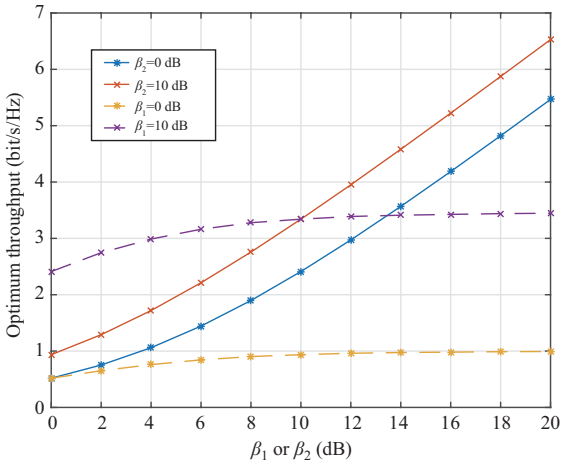

Figure 5 (Color online) The achieved maximum throughput vs. β_1 or β_2 when $\eta = 0.3$ in instantaneous transmission.

as well. The BER decreases when η, β_1 or β_2 increase, as expected. Again, on the right side of the peak, there is a large part of the BER curves that overlap with each other for different η, showing that the BER is not sensitive to η in this part either. Also, the BER is more sensitive to β_1 than to β_2.

Figure 4 shows the optimized value of ρ. When β_2 is fixed to 0 dB or 10 dB, the optimum value of ρ does not change with an increasing β_1. This agrees with the discussion from (21) that the optimum ρ does not depend on $|h|^2$. When β_1 is fixed to 0 dB or 10 dB, the optimum value of ρ decreases with an increase of β_2, as less power needs to be harvested when the channel condition of the relay-to-destination link improves, under the same other conditions. Figure 5 shows the achieved maximum throughput in this case. The maximum throughput increases significantly when β_1 increases for fixed β_2, while it approaches an upper limit when β_2 increases for fixed β_1.

Figures 6–8 show the performances of delay- or error-constrained transmissions. Figure 6 gives the throughput vs. ρ for different values of R_0 and η. Again, there exists an optimum value of ρ that maximizes the throughput, as a larger ρ gives larger energy for harvesting but smaller energy for decoding, which was also observed in the literature. In this case, the throughput decreases when R_0 increases or when η increases. However, when $R_0 = 3$, the throughput does not change with η. Even for $R_0 = 2$, the right side of the peak of the throughput curves largely overlap with each other for different values of η.

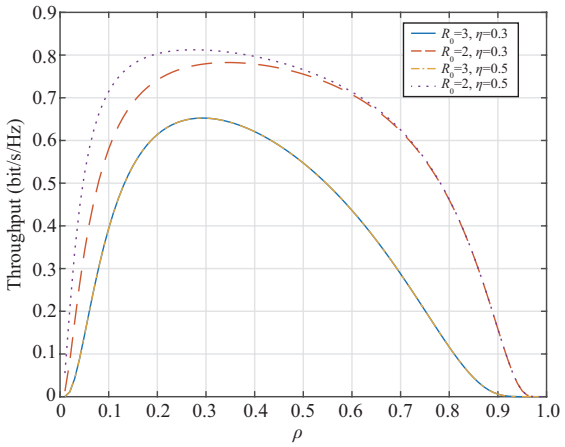

Figure 6 (Color online) Throughput vs. ρ for different values of η, R_0 when $m_1 = m_2 = 2$ in delay-constrained transmission.

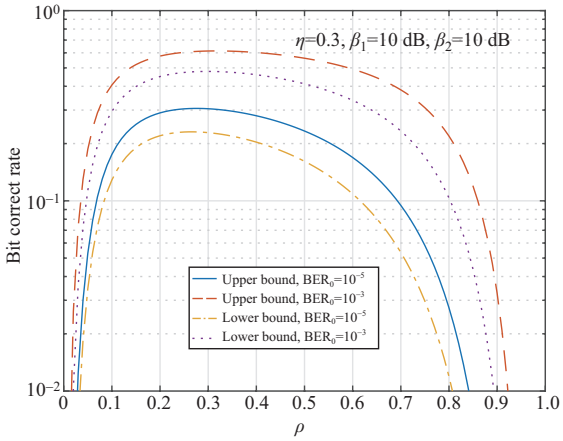

Figure 7 (Color online) BCR vs. ρ for different values of BER_0 and different bounds when $\eta = 0.3$ and $m_1 = m_2 = 2$ in error-constrained transmission.

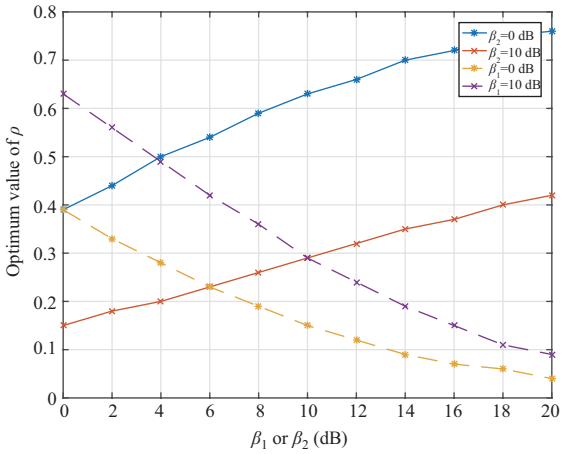

Figure 8 (Color online) The optimum value of ρ vs. β_1 or β_2 when $m_1 = m_2 = 2$, $\eta = 0.3$ and $R_0 = 3$ for the maximum throughput in delay-constrained transmission.

This shows that the throughput is not sensitive to η in delay-constrained transmission. Figure 7 shows the BCR vs. ρ for different values of BER_0 and different bounds of γ_{eq}. In general, the upper bound leads to higher BCR but the optimum value of ρ is approximately the same for both bounds. Figure 8 shows the optimized value of ρ for different values of β_1 and β_2 to achieve the maximum throughput. Since the optimized values of ρ for throughput and BCR are the same, only the throughput results are given. One sees that the optimum value of ρ increases with β_1 for fixed β_2, and it decreases with β_2 for fixed β_1. There is a crossing point between them, implying that the same optimum value of ρ could be achieved by mixing β_1 and β_2 in at least two different ways.

Figures 9–12 show the performances of delay- or error-tolerant transmissions where the ergodic capacity or average BER are considered. Figures 9 and 10 show the throughput and BER vs. ρ for different values of Nakagami-m parameter and η, respectively. Again, an optimum value of ρ exists that either maximize the throughput or minimizes the BER. The throughput also increases when the m parameter increases or when η increases, as they give better channel conditions or higher conversion efficiency, respectively. However, from the figure, it is more sensitive to the m parameter than to η. The optimum value of ρ decreases when m parameter increases or η increases. Similar observations can be made for the BER. In this case, the BER is even less sensitive to η than the throughput.

Figure 11 shows the optimized ρ that achieves the maximum throughput for different values of β_1 and

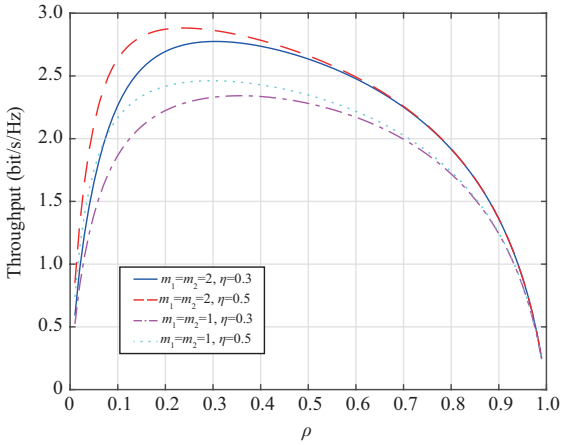

Figure 9 (Color online) Throughput vs. ρ for different values of Nakagami-m parameter and η in delay-tolerant transmission.

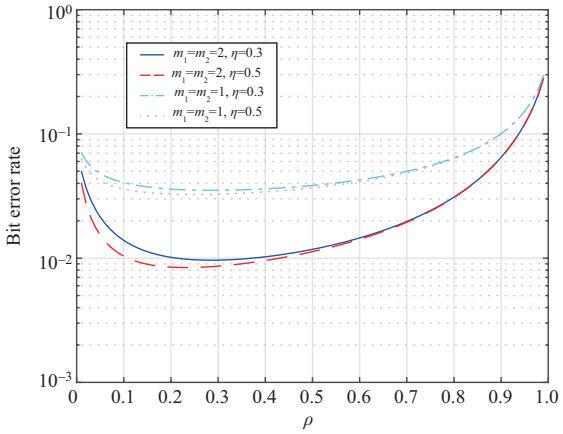

Figure 10 (Color online) BER vs. ρ for different values of Nakagami-m parameter and η in error-tolerant transmission.

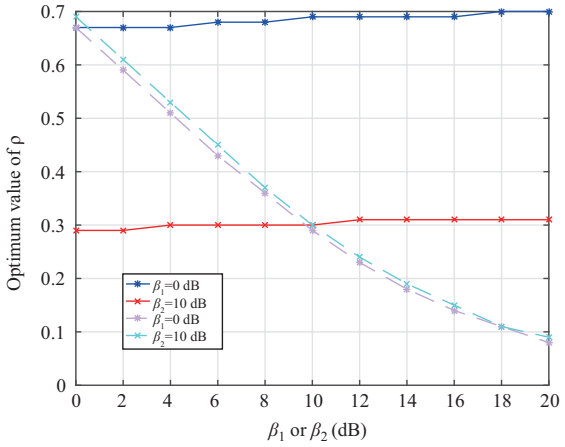

Figure 11 (Color online) The optimum value of ρ vs. β_1 or β_2 when $m_1 = m_2 = 2$ and $\eta = 0.3$ for the maximum throughput in delay-tolerant transmission.

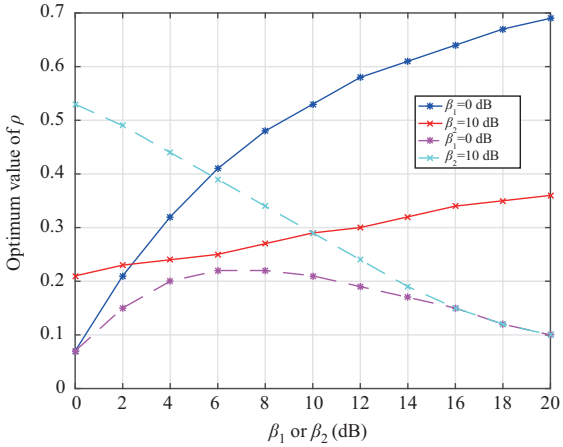

Figure 12 (Color online) The optimum value of ρ vs. β_1 or β_2 when $m_1 = m_2 = 2$ and $\eta = 0.3$ for the minimum BER in error-tolerant transmission.

β_2. Interestingly, in this case when β_2 is fixed to 0 dB or 10 dB, the optimum value of ρ increases very slowly when the value of β_1 increases, although it is not a constant as in the instantaneous transmission. On the other hand, the optimum value of ρ does decrease when the value of β_2 increases, for fixed β_1. This suggests that in delay- or error-tolerant transmissions, the quality of the relay-to-destination link is important. Figure 12 shows the optimized ρ used to calculate the minimum BER in Figure 10 for different values of β_1 and β_2. In this case, this value generally changes significantly when the values of β_1 or β_2 change. However, when β_1 and β_2 are large, the change of the optimum value of ρ is relatively smaller.

Next, we focus on the effect of path loss. To do this, we have to separate d_r^v and d_s^v from β_1 and β_2 that determines the overall performance. Thus, we let $\sigma_{ra}^2 = \sigma_{rc}^2 = \sigma_{da}^2 = \sigma_{dc}^2 = 1$ and $|h|^2/\left(\sigma_{ra}^2 + \sigma_{rc}^2\right) = |g|^2/\left(\sigma_{da}^2 + \sigma_{dc}^2\right) = 10$ dB. Figure 13 shows the effect of path loss. As can be seen, the optimum value of ρ that minimizes the throughput in (21) increases when the distance d_r increases. This agrees with the observation from Figure 4, as the path loss increases when the distance d_r increases and hence the signal power in β_1 decreases. Also, one sees that the optimum ρ increases when v increases, as a larger v incurs a larger path loss. Finally, the optimum ρ increases when η decreases, as more energy needs to be harvested when the efficiency decreases. Figure 14 shows the effect of path loss on throughput. It is clear

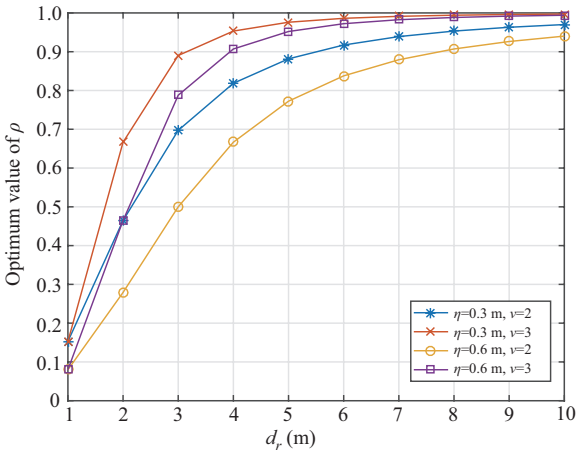

Figure 13 (Color online) The optimum value of ρ in (21) vs. d_r for the maximum throughput in instantaneous transmission for different path loss parameters.

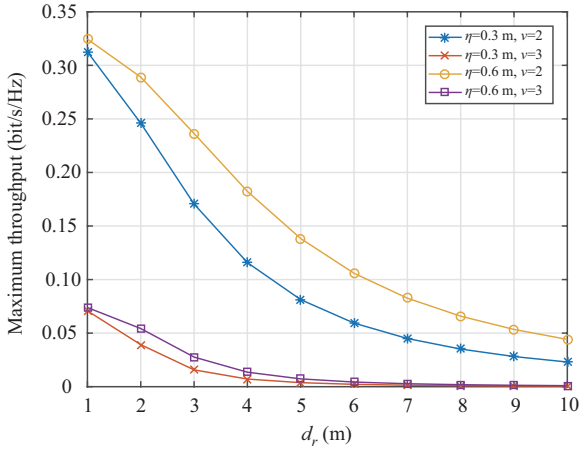

Figure 14 (Color online) The achieved maximum throughput vs. d_r in instantaneous transmission for different path loss parameters.

that the throughput decreases when the path loss increases for large values of the distance, as expected.

5 Conclusion

In this paper, the throughput and the BER of the DF relaying system have been analyzed for Nakagami-m fading channels using PS wireless power. Three different transmission scenarios have been studied. Several important findings can be made. First, for instantaneous transmission, the throughput and BER are not sensitive to the conversion efficiency, when the PS factor is chosen to be larger than its optimum value. Also, the throughput and BER performances improve when β_1 or β_2 increase, and β_1 is more important than β_2. The optimum PS factor does not depend on β_1 at all. Second, for delay- or error-constrained transmission, the throughput increases when the required rate decreases or the conversion efficiency decreases. However, the throughput is not sensitive to the conversion efficiency, especially when the PS factor is larger than its optimum value. In contrast, the BCR performance is sensitive to both the required rate and the conversion efficiency but the upper bound and lower bound of the BCR have similar values of the optimum PS factor, giving us flexibility in system designs. The optimum values of the PS factor are the same for both throughput and BCR, which increases with β_1 and decreases with β_2. This leads to a crossing point where one may choose different combinations of link qualities for the same performance. Third, for delay- or error-tolerant transmission, the throughput increases when the m parameter or the conversion efficiency increase. Again, both throughput and BER are not sensitive to the conversion efficiency, especially for large values of the PS factor. For throughput, the optimum PS factor changes little when β_1 increases while it decreases when β_2 increases. Thus, the relay-to-destination link is more important in this transmission scenario than the other two. In all the cases, there exists an optimum PS factor so that it is important to use our results for guidance. It is noted that this paper assumes simultaneous wireless information and power transfer (SWIPT) relaying where the relay harvests energy from the source node in the system. Non-SWIPT relaying has also been studied in the literature, where the relay harvests energy from ambient sources, such as solar and wind power [20]. This is not the focus of our work.

Acknowledgements The work of Yan Gao was financially supported by Open Foundation of Engineering Research and Development Center for Nanjing College of Information Technology (Grant No. KF20150104), Research Project of Nanjing College of Information Technology (Grant No. YK20150102), Top-notch Academic Programs Project of Jiangsu Higher Education Institutions (Grant No. PPZY2015C242). The work of Aiqun Hu was supported in part by National Natural Science Foundation of China (Grant No. 61571110).

Conflict of interest The authors declare that they have no conflict of interest.

References

1 Laneman J N, Tse D N C, Wornell G W. Cooperative diversity in wireless networks: efficient protocols and outage behaviors. IEEE Trans Inform Theory, 2004, 50: 3062–3080
2 Zhang R, Ho C K. MIMO broadcasting for simultaneous wireless information and power transfer. IEEE Trans Wirel Commun, 2013, 12: 1989–2001
3 Ding Z G, Krikidis I, Sharif B, et al. Wireless information and power transfer in cooperative networks with spatially random relays. IEEE Trans Wirel Commun, 2014, 13: 4440–4453
4 Nasir A A, Zhou X Y, Durrani S, et al. Throughput and ergodic capacity of wireless energy harvesting based DF relaying network. In: Proceedings of IEEE International Conference on Cummunications, Sydney, 2014. 4066–4071
5 Ding Z G, Zhong C J, Ng D W K, et al. Applications of smart antenna technologies in simultaneous wireless information and power transfer. IEEE Commun Mag, 2015, 53: 86–93
6 Gu Y J, Aissa S. RF-based energy harvesting in decode-and-forward relaying systems: ergodic and outage capacities. IEEE Trans Wirel Commun, 2015, 14: 6425–6434
7 Zhang J L, Pan G F. Outage analysis of wireless-powered relaying MIMO systems with non-linear energy harvesters and imperfect CSI. IEEE Access, 2016, 4: 7046–7053
8 Benkhelifa F, Salem A S, Alouini M S. Rate maximization in MIMO decode-and-forward communications with an EH relay and possibly imperfect CSI. IEEE Trans Commun, 2016, 64: 4534–4549
9 Liu H, Kim K J, Kwak K S, et al. Power splitting-based SWIPT with decode-and-forward full-duplex relaying. IEEE Trans Wirel Commun, 2016, 15: 7561–7577
10 Ju M C, Kang K M, Hwang K S, et al. Maximum transmission rate of PST/TSR protocols in wireless energy harvesting DF-based relay networks. IEEE J Sel Area Commun, 2015, 33: 2701–2717
11 Fang B, Zhong W, Jin S, et al. Game-theoretic precoding for SWIPT in the DF-based MIMO relay networks. IEEE Trans Veh Technol, 2016, 65: 6940–6948
12 Liu P, Gazor S, Kim I M, et al. Energy harvesting noncoherent cooperative communications. IEEE Trans Wirel Commun, 2015, 14: 6722–6737
13 Mao M H, Cao N, Chen Y F, et al. Multi-hop relaying using energy harvesting. IEEE Wirel Commun Lett, 2015, 4: 565–568
14 Peng M G, Liu Y, Wei D Y, et al. Hierarchical cooperative relay based heterogeneous networks. IEEE Wirel Commun, 2011, 18: 48–56
15 Zhou B, Hu H L, Huang S Q, et al. Intracluster device-to-device relay algorithm with optimal resource allocation. IEEE Trans Veh Technol, 2013, 62: 2315–2326
16 Gradshteyn I S, Ryzhik I M. Table of Integrals, Series and Products. 7th ed. London: Academic Press, 2007
17 Simon M K, Alouini M S. Digital Communication over Fading Channels. 2nd ed. New York: Wiley, 2005
18 Wang T R, Cano A, Giannakis G B, et al. High-performance cooperative demodulation with decode-and-forward relays. IEEE Trans Commun, 2007, 55: 1427–1438
19 Wang K Z, Chen Y F, Alouini M S, et al. BER and optimal power allocation for amplify-and-forward relaying using pilot-aided maximum likelihood estimation. IEEE Trans Commun, 2014, 62: 3462–3475
20 Medepally B, Mehta N B. Voluntary energy harvesting relays and selection in cooperative wireless networks. IEEE Trans Wirel Commun, 2010, 9: 3543–3553

Appendix A Derivation of (29)

In this appendix, the ergodic capacity of the DF relaying system will be derived. From (28), one has

$$\begin{aligned}\bar{C}=&\int_0^\infty\int_{\frac{\sigma_{da}^2+\sigma_{dc}^2}{(1-\rho)\sigma_{ra}^2+\sigma_{rc}^2}\frac{1-\rho}{\eta\rho}d_r^v}^\infty \ln\left(1+\frac{(1-\rho)P_S x/d_s^v}{(1-\rho)\sigma_{ra}^2+\sigma_{rc}^2}\right)f_{|h|^2}(x)f_{|g|^2}(y)\mathrm{d}x\mathrm{d}y\\&+\int_0^\infty\int_0^{\frac{\sigma_{da}^2+\sigma_{dc}^2}{(1-\rho)\sigma_{ra}^2+\sigma_{rc}^2}\frac{1-\rho}{\eta\rho}d_r^v}\ln\left(1+\frac{\eta\rho P_S xy/(d_s^v d_r^v)}{\sigma_{da}^2+\sigma_{dc}^2}\right)f_{|h|^2}(x)f_{|g|^2}(y)\mathrm{d}x\mathrm{d}y.\end{aligned}\tag{A1}$$

Since h and g are independent, the first term can be calculated as

$$\begin{aligned}&\int_0^\infty\int_{\frac{\sigma_{da}^2+\sigma_{dc}^2}{(1-\rho)\sigma_{ra}^2+\sigma_{rc}^2}\frac{1-\rho}{\eta\rho}d_r^v}^\infty \ln\left(1+\frac{(1-\rho)P_S x/d_s^v}{(1-\rho)\sigma_{ra}^2+\sigma_{rc}^2}\right)f_{|h|^2}(x)f_{|g|^2}(y)\mathrm{d}x\mathrm{d}y\\&=\int_0^\infty\ln\left(1+\frac{(1-\rho)P_S x/d_s^v}{(1-\rho)\sigma_{ra}^2+\sigma_{rc}^2}\right)f_{|h|^2}(x)\mathrm{d}x\cdot\int_{\frac{\sigma_{da}^2+\sigma_{dc}^2}{(1-\rho)\sigma_{ra}^2+\sigma_{rc}^2}\frac{1-\rho}{\eta\rho}d_r^v}^\infty f_{|g|^2}(y)\mathrm{d}y.\end{aligned}\tag{A2}$$

Using the CDF of $|g|^2$ and $W(\cdot,\cdot,\cdot)$ solved in (30) using a variable transformation of $t=1+ax$ and [16, Eq. (4.358.1)], one has (29).

Appendix B Derivation of (33)

The key to derive (33) is to solve two integrals as

$$U(a,b,c)=\int_0^\infty \operatorname{erfc}\left(\sqrt{ax}\right)x^{b-1}\mathrm{e}^{-cx}\mathrm{d}x, \tag{B1}$$

$$V(a,b_1,c_1,b_2,c_2)=\int_0^\infty \operatorname{erfc}\left(\sqrt{axy}\right)x^{b_1-1}\mathrm{e}^{-c_1x}y^{b_2-1}\mathrm{e}^{-c_2y}\mathrm{d}x\mathrm{d}y. \tag{B2}$$

For $U(a,b,c)$, by letting $\sqrt{x}=t$, one has

$$\begin{aligned}U(a,b,c) &= 2\int_0^\infty \operatorname{erfc}\left(\sqrt{a}t\right)t^{2b-1}\mathrm{e}^{-ct^2}\mathrm{d}t=2\int_0^\infty \left[1-\operatorname{erf}(\sqrt{a}t)\right]t^{2b-1}\mathrm{e}^{-ct^2}\mathrm{d}t\\ &= \frac{\Gamma(b)}{c^b}-2\int_0^\infty \operatorname{erf}\left(\sqrt{a}t\right)t^{2b-1}\mathrm{e}^{-ct^2}\mathrm{d}t,\end{aligned} \tag{B3}$$

where $\operatorname{erf}(\cdot)$ is the error function given by $\operatorname{erf}(x)=1-\operatorname{erfc}(x)$. Then, using Eq. (4.3.8) in Geller's work[1)], (34) can be derived. For $V(a,b_1,c_1,b_2,c_2)$, using (34) for the inner integral over x, one has

$$\begin{aligned}V(a,b_1,c_1,b_2,c_2) &= \frac{\Gamma(b_1)\Gamma(b_2)}{c_1^{b_1}c_2^{b_2}}-\frac{2\sqrt{\frac{a}{\pi}}(c_1/a)^{b_2+0.5}}{c_1^{b_1+0.5}}\\ &\quad \int_0^\infty t^{b_2-0.5}\mathrm{e}^{-\frac{c_1c_2}{a}t}{}_2F_1(0.5,b_1+0.5;1.5;-t)\mathrm{d}t.\end{aligned} \tag{B4}$$

Using [16, Eq. (7.522.1)] in the above, one can derive (35). Using $U(a,b,c)$ and $V(a,b_1,c_1,b_2,c_2)$, one has (33).

1) Geller A, Ng E W. A table of integrals of the error functions. J Res Nation Bur Stand, 1969, 73B: 1–20